Early, nonciliary role for microtubule proteins in left–right patterning is conserved across kingdoms

Maria Lobikin[a,b], Gang Wang[c], Jingsong Xu[c], Yi-Wen Hsieh[d], Chiou-Fen Chuang[d], Joan M. Lemire[a,b], and Michael Levin[a,b,1]

[a]Center for Regenerative and Developmental Biology, and [b]Department of Biology, Tufts University, Medford, MA 02155; [c]Departments of Dermatology and Pharmacology, University of Illinois College of Medicine, Chicago, IL 60612; and [d]Division of Developmental Biology, Cincinnati Children's Hospital Research Foundation, Cincinnati, OH 45229

Edited* by Clifford J. Tabin, Harvard Medical School, Boston, MA, and approved June 19, 2012 (received for review February 14, 2012)

Many types of embryos' bodyplans exhibit consistently oriented laterality of the heart, viscera, and brain. Errors of left–right patterning present an important class of human birth defects, and considerable controversy exists about the nature and evolutionary conservation of the molecular mechanisms that allow embryos to reliably orient the left–right axis. Here we show that the same mutations in the cytoskeletal protein tubulin that alter asymmetry in plants also affect very early steps of left–right patterning in nematode and frog embryos, as well as chirality of human cells in culture. In the frog embryo, tubulin α and tubulin γ-associated proteins are required for the differential distribution of maternal proteins to the left or right blastomere at the first cell division. Our data reveal a remarkable molecular conservation of mechanisms initiating left–right asymmetry. The origin of laterality is cytoplasmic, ancient, and highly conserved across kingdoms, a fundamental feature of the cytoskeleton that underlies chirality in cells and multicellular organisms.

C. elegans | *Xenopus* | symmetry breaking

Consistent laterality is a fascinating aspect of embryonic development and has considerable implications for the physiology and behavior of the organism. Although vertebrates are generally bilaterally symmetric externally, most internal organs, such as the heart, viscera, and brain display asymmetric structure and/or unilateral positioning with respect to the left–right (LR) axis. A common defect in LR patterning is the loss of concordance among the sidedness of individual organs known as heterotaxia. In human beings, abnormalities in the proper development of laterality occur in more than 1 in 8,000 live births and often have significant medical consequences (1). Organ asymmetry is highly conserved among species; however, considerable controversy exists about the early steps of LR patterning among phyla (2–4) and the physical mechanisms that can break symmetry (5).

One model predicts that cilia-driven extracellular fluid flow during gastrulation is the origin of LR asymmetry (6). Because numerous species initiate asymmetry before (or without) the presence of cilia (7, 8), this model implies that asymmetry generation must be poorly conserved, with numerous distinct mechanisms used throughout phyla. However, "ciliary" proteins, such as *left–right dynein*, known to be important for LR patterning, also have intracellular roles compatible with cilia-independent functions in laterality (9–12). In contrast to the nodal flow model, we have suggested that asymmetry is instead an ancient, well-conserved property of individual cells arising from the chirality of cytoskeletal structures that is subsequently amplified by physiological mechanisms (4, 12, 13). Thus, we sought the most evolutionarily distant model systems, and ones that are known not to rely on cilia for LR patterning, to test the hypothesis of fundamental molecular conservation of asymmetry mechanisms.

Recent findings in *Arabidopsis thaliana* have shown that mutations in α-tubulin and in a γ-tubulin-associated protein (Tubgcp2) play an important role in the symmetry properties of the plant's axial organs (14–16). Wild-type *A. thaliana* axial organs do not twist during normal elongation, and its flowers are radially symmetrical. This symmetry can be broken by mutations in tubulin and tubulin-associated protein complexes. The tubulin mutations *spiral1*, *spiral2*, and *spiral 3* produce right-handed helical growth mutants. *Lefty* (*lefty1* and *lefty2*) mutants were found to be suppressor mutants of *spiral1*, and when outcrossed displayed a prominent left-handed helical growth (14, 16). Both α-tubulin and γ-tubulin complexes are ubiquitous in eukaryotes and are involved in the formation and nucleation of microtubules. Here, we characterize the laterality phenotypes induced by the same mutations in a vertebrate (the frog *Xenopus laevis*), the nematode *Caenorhabditis elegans*, and mammalian cells, supporting a fundamental role for tubulin in the cilia-independent generation of LR asymmetry.

Results

To determine if the same tubulin proteins implicated in *Arabidopsis* asymmetry also control large-scale asymmetry of both vertebrate and plant systems, homologous mutations were made in *X. laevis* α tubulin and γ tubulin-associated protein Tubgcp2 (Fig. S1). These mutations function as dominant negatives when assembled into the cytoskeleton together with native subunits (14, 17). Synthetic mRNAs encoding mutant tubulins were injected into *Xenopus* embryo blastomeres (at various early stages) using standard methods (18). At stage 45, embryos were analyzed for position (situs) of the heart, stomach, and gallbladder (Fig. 1 *A*–*C*), the definitive readout of LR patterning. All treatments were titered to avoid nonspecific defects (resulting in embryos with perfectly normal dorsoanterior development, clear left- or right-sided organs with normal morphology, correct size and relative proportions, and wild-type behavior), ruling out general toxicity as a cause of LR phenotypes.

Embryos injected immediately after fertilization with mRNA encoding the dominant negative mutant α-tubulin (tub4a) displayed significant levels of heterotaxia (independently randomized sidedness of the three scored organs, Figs. 1*D* and *E*), revealing a common genetic underpinning of regulation of asymmetry between plant and vertebrate systems. Injections of wild-type tub4a mRNA had no effect. Co-injections of both mutants' mRNAs together did not significantly increase the incidence of heterotaxia, suggesting that these impact the same pathway (are not additive). We next introduced the mutant mRNAs at

Author contributions: M. Lobikin, G.W., J.X., Y.-W.H., C.-F.C., and M. Levin designed research; M. Lobikin, G.W., J.X., Y.-W.H., and C.-F.C. performed research; M. Lobikin, G.W., J.X., C.-F.C., J.M.L., and M. Levin contributed new reagents/analytic tools; M. Lobikin, G.W., J.X., Y.-W.H., C.-F.C., and M. Levin analyzed data; and M. Lobikin, J.X., C.-F.C., and M. Levin wrote the paper.

The authors declare no conflict of interest.

*This Direct Submission article had a prearranged editor.

Freely available online through the PNAS open access option.

[1]To whom correspondence should be addressed. E-mail: michael.levin@tufts.edu.

This article contains supporting information online at www.pnas.org/lookup/suppl/doi:10.1073/pnas.1202659109/-/DCSupplemental.

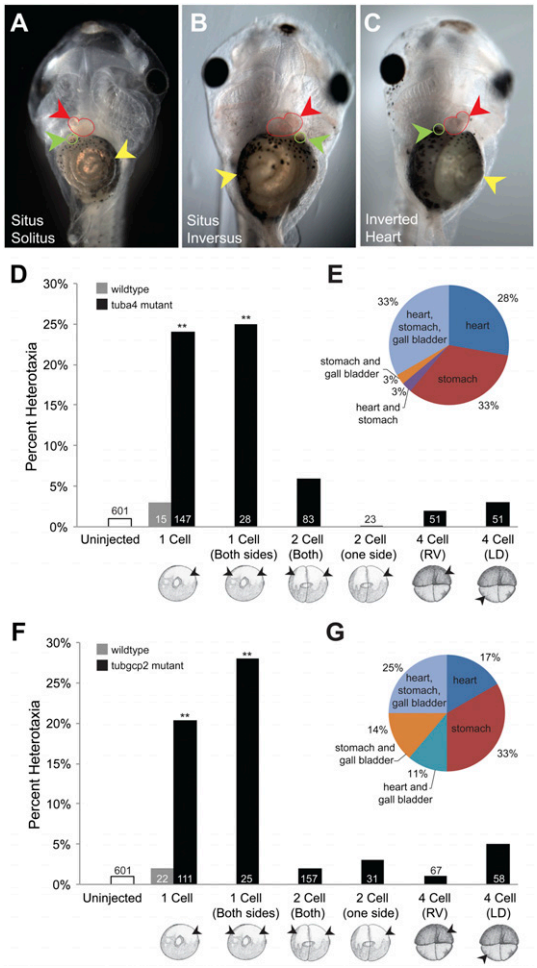

Fig. 1. Tubulin mutations affect LR asymmetry before the first cleavage event. (*A*–*C*) Organ situs of stage 45 embryos scored by observation. (*A*) A wild-type embryo, ventral view, showing the normal arrangement of the stomach (yellow arrowhead), heart apex (red arrowhead), and gall bladder (green arrowhead). (*B*) A heterotaxic embryo (ventral view) showing reversal of all three organs, i.e., situs inversus, induced by misexpression of the tubulin mutant. (*C*) A heterotaxic embryo (ventral view) showing reversal of the heart. (*D*) Statistical comparison of heterotaxia levels scored at stage 45 in embryos injected with mutated α-tubulin mRNA at various early cleavage stages. (*E*) Types of heterotaxia observed from embryos injected with mutated α-tubulin mRNA at the one-cell stage. (*F*) Statistical comparison of heterotaxia levels in embryos injected with mutated Tubgcp2 mRNA at various early cleavage stages. (*G*) Types of heterotaxia observed from embryos injected with mutated Tubgcp2 mRNA at the one-cell stage. $^{**}P < <0.01$, Welch's *t* test, sample sizes as noted in Table S2. For both constructs, it is only the presence before two-cell stage that allows these reagents to randomize laterality.

different time points during development, to determine when the tubulins functioned in LR patterning and test the possibility that the relevant tubulin structures are in the cilia at the gastrocoel roof plate (GRP).

Synthetic mRNAs injected immediately after fertilization are already translated by the two-cell stage (Fig. S2 and ref. 19); studies of GRP cilia routinely inject at the four-cell stage to target reagents to this structure (20). If tubulins were to function in LR asymmetry at any time *after* the first few cleavages (e.g., in the GRP during neurulation), injections at the two- or four-cell stages would show the same randomizing effects on asymmetry as do injections at one-cell stage. In contrast, injections of mutant tub4a mRNA into both blastomeres of the two-cell embryo (or later) had no effect on asymmetry. The mutant tubulin's introduction into very early embryos randomizes LR patterning when present during the earliest events of cleavage-stage development, but cannot affect the LR axis when introduced as early as the two-cell stage, ruling out involvement in LR patterning steps occurring after the first cleavages.

The *Xenopus* fate map facilitates targeting to the right or left halves of the embryo (Fig. S3), allowing us to test spatial requirements for tubulin mutant-induced randomization with respect to the ciliated organ. Targeted injections were made in four-cell stage embryos, in the left-dorsal (LD) blastomere, which is known to be an early precursor of the GRP and the only side required for nodal flow (20), or the right-ventral (RV) cell, whose descendants do not contribute to the GRP (21). Neither injection made at the four-cell stage produced significant levels of heterotaxia (Fig. 1*D*), a result incompatible with mutant α-tubulin affecting asymmetry via impact upon cilia-related events at the node. The same results were obtained using injections of mRNA encoding mutated γ-tubulin associated protein (tubgcp2) mRNA (Fig. 1 *F* and *G*). For both constructs, a single injection or two injections 180° apart at the one-cell stage randomized laterality, but injections of both or a single blastomere at the two-cell stage or later did not, ruling out the possibility that effects at the one-cell stage are due to an imbalance of injected mRNA on one side but not the other. These data reveal that the same functions of tubulin that alter asymmetry in a plant species are also involved in LR patterning in frog embryos, and that this function takes place at or just before the first cleavage.

To determine whether the tubulin-regulated events function in the same pathway as known early LR mechanisms and control downstream asymmetric transcription, we asked whether the expression of tubulin mutants perturbed the normally left-sided expression of the earliest known asymmetric gene in *Xenopus*: the TGF-β signaling factor Nodal (Xnr-1) (22). Xnr-1 is normally expressed only on the left side of the embryo at approximately stage 22 (23). Embryos injected with mutated tubulin mRNAs at the one-cell stage were fixed at stage 22 and processed for in situ hybridization with an *Xnr-1* probe. A significant percentage (64.7% for tub4a and 32.5% for tubgcp2) of mutant-injected embryos displayed incorrect *Xnr-1* expression (Fig. 2), showing that these tubulin mutations affect LR asymmetry upstream of *Nodal* expression.

One model is that mutant tubulins perturb the normal rightward bias in the intracellular transport provided by the cytoskeleton in cleavage-stage frog embryos (19, 24). These oriented cytoskeletal tracks allow cytoplasmic motors, such as kinesins and dyneins, to localize specific protein cargo to the left or right sides. We previously showed that the cytoskeleton during the one-cell stage confers rightward bias to kinesin heavy chain (KHC) motors and their cargo (25–27). We asked whether this aspect of the normal *Xenopus* cytoskeleton might be perturbed following the misexpression of our mutant proteins. Embryos were injected at the one-cell stage with mRNA encoding KHC fused to a β-gal reporter protein, and sectioned at the four-cell stage to quantify the distribution of β-gal (blue) signal on the left vs. right sides; this assay (28) provides a readout of the cytoskeletal orientation via localization of the microtubule-dependent motor protein KHC (Fig. 3*A*). Embryos receiving β-gal alone (which cannot localize by intracellular transport) most often exhibited bilateral signal. As previously described, β-gal:KHC fusions were preferentially localized on the right; crucially, the localization of β-gal:KHC signal in embryos also injected with the tubgcp2 mutant became disrupted, and exhibited approximately equal number of right, left, and bilateral localizations for the KHC motor and its cargo (Fig. 3 *B* and *C*). The difference in localization of microtubule-dependent motor protein cargo between these three conditions was statistically significant ($P < 0.01$, χ^2), confirming that the introduction of the tubgcp2 mutant alters a known aspect of early microtubule

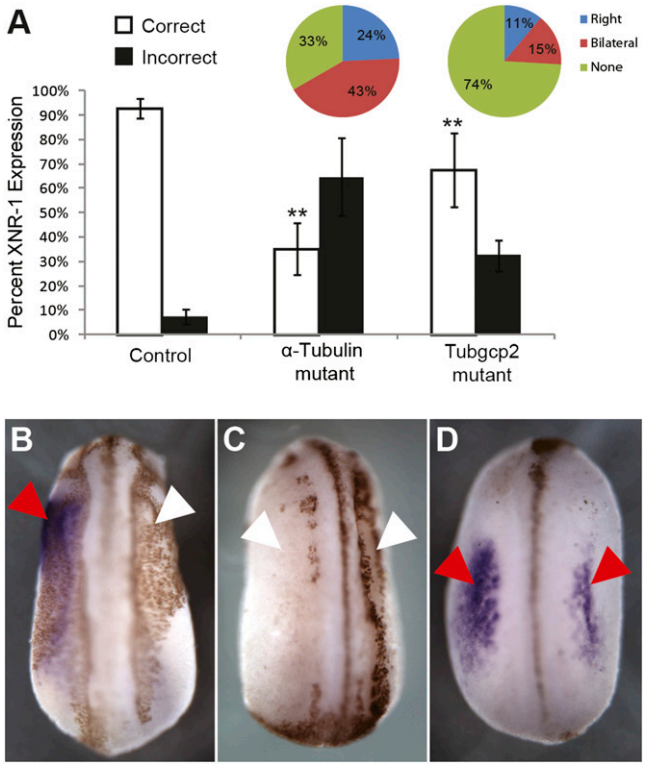

Fig. 2. Tubulin mutations perturb sidedness of asymmetric gene expression in *Xenopus*. Embryos injected with either tub4a mutant or Tubgcp2 mutant were processed for in situ hybridization at stage 22 with an Xnr-1 probe. (*A*) Both tubulin mutants deviated significantly (denoted with double asterisks) from control embryos (Tub4a: 64.7% incorrect expression, $n = 51$, $P < <0.01$ Welch's t test; Tubgcp2: 32.5% incorrect expression, $n = 83$; control: 7.33% incorrect expression, $n = 150$, $P < <0.01$ Welch's t test). (*B–D*) Xnr-1 expression pattern (purple stain) characterized in tubulin mutant mRNA-injected embryos. (*B*) Left expression indicated by one red arrow and one white arrow. (*C*) Absence of expression as indicated by two white arrows. (*D*) Bilateral expression as indicated by two red arrows.

function. Interestingly, β-gal signal was almost never detected in embryos when the tuba4 mutant was coinjected with the β-gal:KHC (109 out of 110 embryos); although this remains to be investigated in future studies, it is conceivable that some new aspect of cytoskeletal organization can also trigger protein degradation machinery for molecular motors' cargo.

Having shown an alteration in cytoskeletal organization and a mislocalization of previously described asymmetric transport, we next sought a comprehensive (unbiased) analysis of asymmetric maternal components in the early embryo, and wanted to determine which of these were dependent on tubulin (thus identifying also those asymmetric *Xenopus* proteins for which no immunohistochemistry-suitable antibody is available). We performed a quantitative proteomics profiling of the left and right sides of four-cell embryos. Control embryos, and those injected at the one-cell stage with either the tub4a or tubgcp2 mutant, were fixed in methanol at the four-cell stage, oriented, and split along the LR axis (first cleavage plane) with a blade. The left and right sides were pooled ($n = 50$), and samples were analyzed via liquid chromatography-mass spectrometry. Proteins showing a significant ($P < 0.05$, ANOVA) (more than 3× difference in either direction) left- or right-sided bias in control embryos were selected. The analysis confirmed asymmetric localization of ion transporters (Tables S3 and S4) and the higher frequency of right-biased targets, which has been noted in previous work (19, 26, 27). The presence of mutated tubulin significantly affected the endogenous bias in localization of some proteins, either reversing or completely abolishing it (Tables S3 and S4). As expected, this included cytoskeletal and transport-related proteins such as dynactin, cofilin-1, and a nonmuscle myosin (Table S1).

Cofilin-1, an actin depolymerization and filament severing protein (29), was chosen for further investigation because of the known importance of actin in early cytoskeletal organization, Cofilin's role in directing the intracellular trafficking of ion transporter cargo (30), and recent data showing cofilin is asymmetrically transcribed in the two-cell mouse embryo (31). Fertilized eggs injected with either tdTomato:Cofilin-1a alone, or in conjunction with a tubulin mutant, were allowed to develop and analyzed for tdTomato localization (Fig. 4) at stage 45, where the embryo's transparency allowed clear detection of which side's progenitor cells had inherited the tagged cofilin. Whereas injections of tdTomato alone showed no significant bias in localization, tdTomato:Cofilin-1a injections revealed a significant ($P << 0.01$, paired t test) leftward bias in the fluorescent signal (Left localized: Right localized ratio, L:R, of 1.35), confirming that cofilin protein is indeed localized asymmetrically during the first cleavages. Coinjections of either tubulin mutant together with the tdTomato:cofilin-1a significantly ($P < 0.05$)

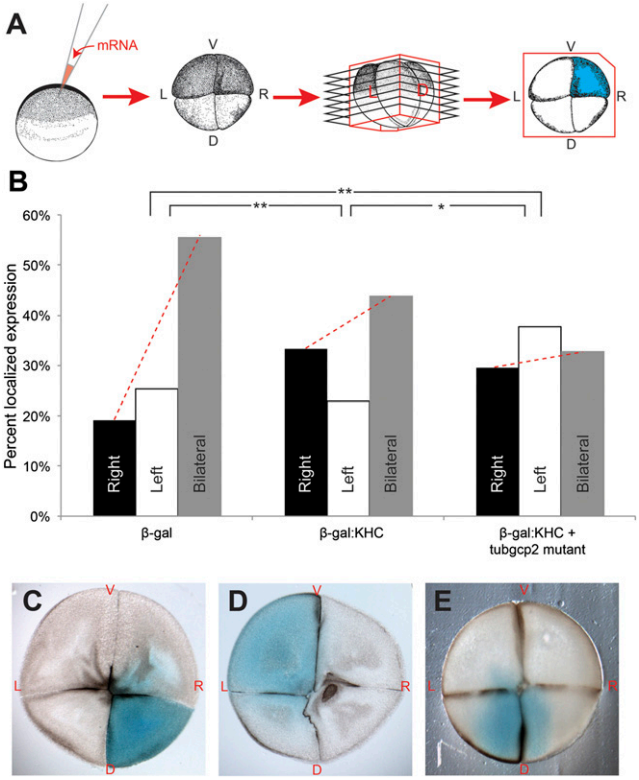

Fig. 3. Tubulin mutations affect early microtubule-dependent motor protein transport. (*A*) Embryos were injected into the very top of the animal pole shortly after fertilization with either a control β-gal mRNA, mRNA encoding the β-gal:KHC motor protein fusion construct or a mixture of β-gal:KHC and mutated tubgc2. At the four-cell stage, embryos were fixed and processed for β-gal staining then embedded with consistent LR orientation, sectioned and scored for localization of the blue stain in the blastomeres as described (19). (*B*) Control embryos, injected with β-gal mRNA, displayed little LR bias (19% right, 25% left, 56% bilateral), whereas embryos that had been injected with β-gal:KHC displayed a significant rightward bias in β-gal localization (33% right, 23% left, 44% bilateral). Coinjections of tubgcp2 with the β-gal:KHC reversed this rightward bias (30% right, 38% left, 33% bilateral). $*P < 0.05$, $**P < 0.01$, χ^2 test. (*C–E*) Typical β-gal expression patterns observed in sectioned four-cell embryos.

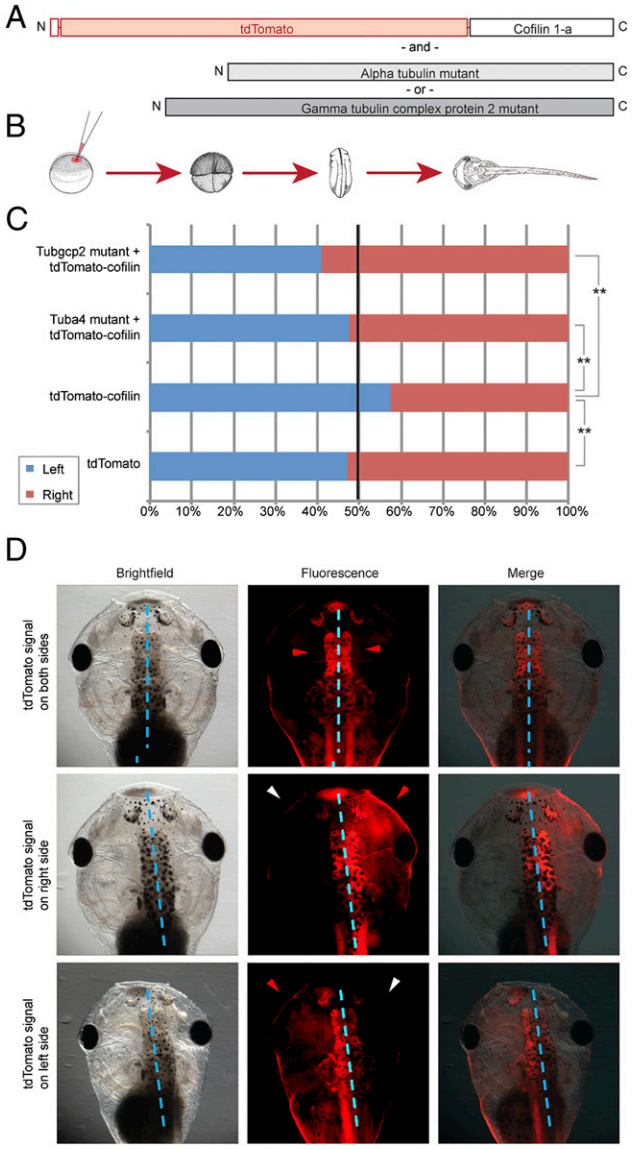

Fig. 4. Tubulin mutations alter biased Cofilin-1 expression. (*A*) tdTomato:Cofilin-1a fusion mRNA was injected into *Xenopus* embryos either alongside tub4a mutant mRNA, tubgcp2 mutant mRNA or on its own. (*B*) Injections were made shortly after fertilization; embryos were reared to stage 45 before scoring for tdTomato fluorescent signal. (*C*) Control embryos, injected with solely the tdTomato fluorescent marker displayed virtually no bias for signal localization (left localized:right localized ratio, L:R = 0.89, n = 117), whereas tdTomato:Cofilin-1a injected embryos displayed a leftward bias (L:R ratio = 1.35, n = 192). Embryos that had been coinjected with the tdTomato:Cofilin-1a and a tubulin mutant (either tub4a or tubgcp2) resulted in reversals in this bias (0.91 L:R ratio in tub4a mutant, n = 127; L:R ratio = 0.69 in tubscp2 mutant, n = 208). Blue dashed line indicates embryo midplane. (*D*) tdTomato expression patterns observed in stage 45 *Xenopus* embryos. *$P < 0.05$; **$P < 0.01$.

altered the normal left-ward bias of cofilin localization, and lead to subsequent randomization of organ situs (Fig. S4 and Table S5). Coinjection with the tuba4 mutant resulted in a 0.91 L:R bias, thus abolishing cofilin's leftward bias, whereas the tubgcp2 mutant resulted in a 0.69 L:R ratio, reversing the bias (Fig. 4 *C* and *D*). Scoring organ situs in tdTomato:cofilin-injected embryos revealed a weak but significant (8%) incidence of heterotaxia, consistent with some impairment of the interaction of cofilin with the LR localization machinery due to the addition of a large tdTomato structure (thus likely artificially lowering the bias in localization we observed). Thus, tubulin mutations are perturbing the normal consistent LR bias of a range of maternal proteins at the four-cell stage, consistent with models in which cytoskeletal organization drives positioning of LR-relevant cargo during the first cleavages.

Having observed the remarkable conservation of asymmetry roles for tubulin proteins between frog and *Arabidopsis*, we tested the same mutations in two additional model systems: the nematode *C. elegans*, and human HL-60 cells, thereby covering an extremely broad range of asymmetry types and bodyplans.

The two "AWC" olfactory neurons of *C. elegans* are morphologically symmetric, but display asymmetric expression of chemosensory receptors along the LR axis. Wild-type animals generate one AWC^{ON} cell, which expresses the reporter gene *str-2p::GFP*, and one AWC^{OFF} cell, which does not (Fig. 5 *A–C*) (32). Specific disruption of microtubules in AWC by nocodazole and benomyl generates two AWC^{ON} neurons, suggesting that microtubules are required for LR AWC neuronal asymmetry (33). *C. elegans* TBA-9 α-tubulin shares 75% identical amino acids with *A. thaliana* TUA6 α-tubulin. We mutated the conserved aspartic acid (256th) and glutamic acid (259th) residues in

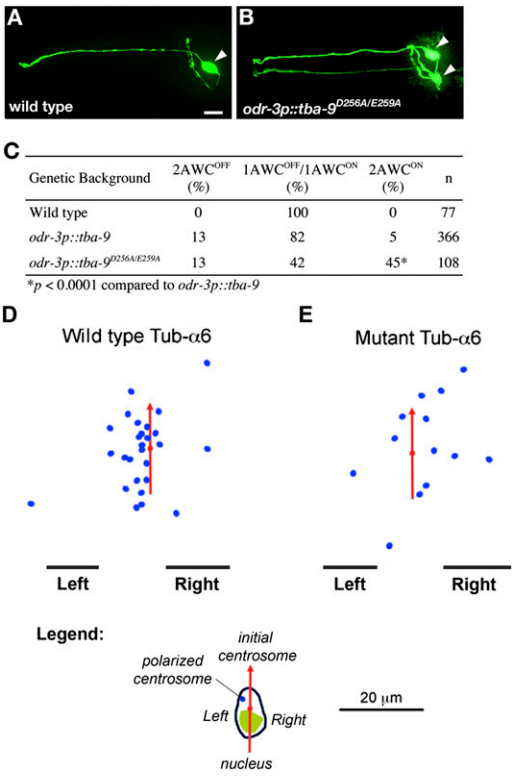

Fig. 5. Mutant tubulin disrupts LR asymmetry in *C. elegans* embryos and cultured HL-60 cells. (*A*) Wild-type *C. elegans* generate one AWC^{ON} olfactory neuron cell, which expresses the reporter gene *str-2p::GFP*, and one AWC^{OFF} cell, which does not (32). (*B*) *C. elegans* bearing mutations in aspartic acid (256th) and glutamic acid (259th) residues in α-tubulin exhibit a 2 AWC^{ON} phenotype at a frequency significantly higher than that caused by expression of wild-type TBA-9. These frequencies are quantified in *C*. Differentiated HL-60 cells were transiently cotransfected with GFP-Arrestin-3 (as marker of MTOC) and wild type tub-a6 (*D*) or mutant tub-a6 (*E*), and then exposed to uniform fMLP (100 nM), which induced polarization. The red arrow is drawn through the center of the nucleus, pointing to the centrosome, at 0 s as described (35). Final centrosome positions are indicated by the blue dots, relative to all red arrows coaligned. Whereas wild-type tub-a6 does not affect the leftward bias, mutant tub-a6 abolishes it (χ^2 test, $P <$ 0.01). (Scale bar, 20 μm.)

TBA-9 to alanine and expressed the TBA-9$^{D256A/E259A}$ mutant protein in AWC under the control of the *odr-3* promoter. Like nocodazole treatment, expression of TBA-9$^{D256A/E259A}$ caused a two-AWC^{ON} phenotype at a frequency significantly higher than that caused by expression of wild-type TBA-9 when injected at the same concentration (Fig. 5*C*). Both *odr-3p::tba-9* and *odr-3p::tba-9*$^{D256A/E259A}$ transgenes also caused a weak two-AWC^{OFF} phenotype. Thus, two conserved residues in the GTPase-activating domain of α-tubulins regulate microtubule dynamics required for precise LR patterning of *C. elegans*.

An important recent finding is the observation that mammalian cells in culture, having neither node-like structure nor cilia-derived fluid flow, establish and maintain consistent LR asymmetries with respect to axes defined by internal polarity markers (34, 35). Neutrophil-like HL-60 cells in culture extend pseudopodia to the left of an axis drawn between the nucleus and centrosome (35). To test whether this asymmetry likewise depended on functional tubulin proteins, we transfected differentiated HL-60 cells with GFP-Arrestin-3 (a marker of the microtubule organizing center) and one of the tubulin constructs: wild-type tub-a6 (Fig. 5*D*), or mutant tub-a6 (Fig. 5*E*). Whereas wild-type tub-a6 (at expression levels achievable by transfection) did not affect the leftward bias, mutant tub-a6 abolished it. Thus, the same tubulin mutations that specifically randomize asymmetry in plant, vertebrate, and nematode systems likewise do so in mammalian cells.

Discussion

The ciliary flow paradigm is forced to postulate highly divergent origins of asymmetry, because numerous invertebrate phyla establish consistent LR asymmetry without cilia or a node. Moreover, neither the pig nor the chick use cilia in their LR patterning pathway (8, 36); zebrafish (37–39) and mouse (40) mutants exhibit normal asymmetry despite ciliary defects, and even mouse embryos already have LR-nonequivalent blastomeres by the third cleavage (41). We tested a model of much earlier asymmetry-determining processes that would exhibit a more satisfying evolutionary conservation across a wide range of phyla.

Our data show that the presence of well characterized mutant forms of either α- or γ- tubulin subunits in frog embryos specifically randomizes the LR axis (Fig. 1), controlling the LR pathway upstream of the well conserved asymmetric expression of *Nodal* (Fig. 2). Although the levels of heterotaxia were clearly significantly different from controls, they were below the ~87% theoretical maximum (for three fully randomized organs) because of the need to titer mutant tubulin mRNA to low levels to avoid possibility of confounding pure asymmetry phenotypes with general toxicity. Despite the crucial housekeeping roles of tubulin, we were able to find a level of expression of mutants that allowed dissection of their LR patterning roles independent of any toxicity or generalized teratology.

Varying the time of injection allowed us to place strict bounds on the timing of the activity of these proteins in the LR pathway. Strikingly, whereas one-cell injections (whether made on one or both sides of the prospective midline) randomized asymmetry, injections at the two- or four-cell stage were already too late to do so (Fig. 1 *D* and *F*), suggesting that the function of tubulin in asymmetry occur no later than approximately the four- or eight-cell stage (because two-cell injections produce protein by then). Most crucially, injections of both cells at the two-cell stage do not affect asymmetry, ruling out interference with cilia-driven events at the GRP as the mechanism by which these mutants randomize the LR axis. Because the GRP is strongly affected by reagents injected at four-cell stage (20), our results show that expressing mutant tubulin in GRP cells makes no difference to asymmetry; the key factor that determines whether or not the LR axis will be randomized is whether tubulin mutant mRNA was injected before the two-cell stage and thus was available for translation during the earliest stages of development. The need to function during the first few cleavages (Fig. 1) is incompatible with explanations involving cilia or nodal flow. Instead, the data are consistent with models in which the early cytoskeleton is nucleated by a chiral structure (42) that orients itself with respect to the other two axes, and thus biases the intracellular transport of key determinants along the LR axis (12, 43). One such model is shown in Fig. S5.

As in snail embryos (44), early cytoskeletal dynamics are transduced into changes of asymmetric gene expression in vertebrate embryos. We previously showed that orientation of the cytoskeleton at the first few cleavages is crucial for the correct asymmetric localization of several maternal proteins whose activity is in turn transduced into asymmetric transcription (19, 27, 45); by the second cell cleavage, the cytoskeleton already exhibits a directionality that results in accumulation of kinesin-associated cargo (or marker molecules) to the right side (19). Others showed that a preexisting consistent chirality of the cytoskeleton exists in the egg cortex (46). Despite the reduced levels of mRNA needed for double injections (β-gal:KHC + tubgcp2 mutant), introduction of the mutant tubulin significantly affected the ability of the native cytoskeleton to direct normal localization of motor protein cargo (Fig. 3). We hypothesize that the presence of these mutant tubulin proteins alter subtle aspects of the intracellular cytoskeleton that are required to properly localize laterality-relevant cargo molecules across the LR axis.

To get the first unbiased glimpse of such asymmetries existing very soon after establishment of the midline, we performed a proteomic analysis comparing the left and right blastomeres' contents. This analysis revealed proteins with significant LR bias at the four-cell stage (Tables S3 and S4). Although the functions of these asymmetrically localized proteins remain to be probed by future studies, these data confirm the existence of consistent molecular asymmetries at very early stages (long before gastrulation) (25, 27, 46, 47) and exhibit a relative enrichment of right-sided proteins as found in our previous screens.

Although the large yolky cells of the early frog embryos are not conducive to the high-resolution imaging of cytoskeletal structure needed to identify subtle changes in chirality, the proteomic data reveal the consequences of tubulin mutation for the asymmetric distribution of early embryonic components, despite the unavailability of antibodies. Analysis of protein distribution after microinjection of the two mutant cytoskeletal protein mRNAs showed (Table S1) that a number of important signaling proteins become mislocalized. Thus, we propose that the role of tubulins during early development is to serve as components of the chiral cytoskeleton by means of which asymmetric components sort to the left and right sides during the first cleavages, and as an important component of other intracellular localization events taking place at the two- to eight-cell stages. We selected cofilin, and labeled it with a fused fluorescent protein. Although this had somewhat of a destabilizing effect on asymmetry (Fig. S4, suggesting a possible functional role for cofilin), we were able to observe a statistically significant bias in its native localization (Fig. 4 *C* and *D*) and showed that this native LR bias is abolished when tubulin mutants are introduced in the one-cell embryo.

Our data support previous models in which cytoskeletal chirality is amplified via differences in intracellular transport of key cargo during very early stages (24, 43, 48, 49). Although the details are somewhat different, that same scheme is used by snail (44) and *C. elegans* (33) embryos, and the same initial asymmetry is also compatible with a number of subsequent amplification mechanisms including asymmetric chromatid segregation (9) and planar cell polarity (4). Perhaps the most remarkable aspect of these data is the widespread evolutionary conservation (even across the independent origin of multicellularity in plants and animals) of the role of these tubulin proteins in asymmetry, extending to plant coiling (15), *C. elegans* asymmetric neural

patterning (Fig. 5 *A*–*C*), pseudopodial asymmetries in human cells in culture (Fig. 5 *D* and *E*), and organ placement of the vertebrate *X. laevis* (Fig. 1). These findings are consistent with the nonciliary roles for tubulin in frog asymmetry, as neither nematodes nor plants nor HL-60 cells use cilia in their asymmetry pathways. We have previously stressed the evolutionary conservation of several asymmetry-amplifying mechanisms across multiple diverse taxa (7, 12, 13, 50). The above results implicate a single protein as an ancient, fundamental element with a highly conserved role as the initiator of chirality, upon which very different bodyplans can establish consistent downstream asymmetries of form and function.

Materials and Methods

For frogs, plasmids containing *X. laevis* tuba4 and Tubgcp2 (Xgrip110) and cofilin cDNA were purchased from Open Biosystems (clone IDs: 7010865, 5078639, and 5571290, respectively). The coding regions of these cDNAs were amplified by PCR and inserted into pCS2+ expression vectors using the In-Fusion Advantage PCR Cloning kit (Clontech). Tuba4 pCS2 and TubGCP2 pCS2 plasmids were linearized with Acc65I for SP6 transcription. Tuba4-mut (Ala180 replaced with Phe) and tubgcp2-mut (Gly453 replaced with Arg) were generated using the QuikChange II Site-directed Mutagenesis kit (Stratagene).

For nematodes, full-length *tba-9* cDNA (1368 bp) was obtained with RT-PCR of total mRNA from mixed stage worms and was subcloned to make *odr-3p::tba-9::SL2::TagRFP*. *odr-3p::tba-9*$^{D256A/E259A}$*::SL2::TagRFP* was generated by site-directed mutagenesis (Stratagene QuikChange kit). *odr-3p::tba-9::SL2::TagRFP* (50 ng/μL) and *odr-3p::tba-9*$^{D256A/E259A}$*::SL2::TagRFP* (50 ng/μL) were injected as described (51). The coinjection marker *ofm-1p::DsRed* was injected at 30 ng/μL. Please see *SI Materials and Methods* for additional methods details. All experiments were conducted according to approved protocols (Institutional Animal Care and Use Committee, No. M2008-08).

ACKNOWLEDGMENTS. We thank Claire Stevenson for assistance with molecular biology; Punita Koustubhan and Amber Currier for *Xenopus* husbandry; Erol Gulcicek, Christopher Colangelo, and Thomas Abbott for assistance with interpretation of proteomic data; and Laura Vandenberg and the other members of the M. Levin laboratory for useful discussions. M. Levin acknowledges funding support from National Institutes of Health (NIH) Grant R01-GM077425 and American Heart Association Established Investigator Grant 0740088N; J.X. acknowledges funding support from NIH Grant HL095716; Y.-W.H. was supported by an NIH Training Grant of Organogenesis; and C.-F.C. was supported by a Whitehall Foundation Research Award and an Alfred P. Sloan Research Fellowship.

1. Peeters H, Devriendt K (2006) Human laterality disorders. *Eur J Med Genet* 49: 349–362.
2. Tabin C (2005) Do we know anything about how left-right asymmetry is first established in the vertebrate embryo? *J Mol Histol* 36:317–323.
3. Vandenberg LN, Levin M (2009) Perspectives and open problems in the early phases of left-right patterning. *Semin Cell Dev Biol* 20:456–463.
4. Aw S, Levin M (2009) Is left-right asymmetry a form of planar cell polarity? *Development* 136:355–366.
5. Wolpert L (2009) Diffusible gradients are out - an interview with Lewis Wolpert. Interviewed by Richardson, Michael K. *Int J Dev Biol* 53:659–662.
6. Basu B, Bruedner M (2008) Cilia: Multifunctional organelles at the center of vertebrate left-right asymmetry. *Current Topics in Developmental Biology*, ed Yoder BK (Elsevier Academic, San Diego), Vol 85, pp 151–174.
7. Spéder P, Petzoldt A, Suzanne M, Noselli S (2007) Strategies to establish left/right asymmetry in vertebrates and invertebrates. *Curr Opin Genet Dev* 17:351–358.
8. Gros J, Feistel K, Viebahn C, Blum M, Tabin CJ (2009) Cell movements at Hensen's node establish left/right asymmetric gene expression in the chick. *Science* 324:941–944.
9. Armakolas A, Klar AJ (2007) Left-right dynein motor implicated in selective chromatid segregation in mouse cells. *Science* 315:100–101.
10. Klar AJ (2008) Support for the selective chromatid segregation hypothesis advanced for the mechanism of left-right body axis development in mice. *Breast Dis* 29:47–56.
11. Zhang Y, Levin M (2009) Left-right asymmetry in the chick embryo requires core planar cell polarity protein Vangl2. *Genesis* 47:719–728.
12. Levin M, Palmer AR (2007) Left-right patterning from the inside out: Widespread evidence for intracellular control. *Bioessays* 29:271–287.
13. Vandenberg LN, Levin M (2010) Far from solved: A perspective on what we know about early mechanisms of left-right asymmetry. *Dev Dyn* 239:3131–3146.
14. Abe T, Thitamadee S, Hashimoto T (2004) Microtubule defects and cell morphogenesis in the lefty1lefty2 tubulin mutant of Arabidopsis thaliana. *Plant Cell Physiol* 45:211–220.
15. Thitamadee S, Tuchihara K, Hashimoto T (2002) Microtubule basis for left-handed helical growth in *Arabidopsis*. *Nature* 417:193–196.
16. Nakamura M, Hashimoto T (2009) A mutation in the Arabidopsis gamma-tubulin-containing complex causes helical growth and abnormal microtubule branching. *J Cell Sci* 122:2208–2217.
17. Ishida T, Kaneko Y, Iwano M, Hashimoto T (2007) Helical microtubule arrays in a collection of twisting tubulin mutants of Arabidopsis thaliana. *Proc Natl Acad Sci USA* 104:8544–8549.
18. Sive H, Grainger RM, Harland RM (2000) *Early Development of Xenopus Laevis: A Laboratory Manual* (Cold Spring Harbor Laboratory Press, New York).
19. Aw S, Adams DS, Qiu D, Levin M (2008) H,K-ATPase protein localization and Kir4.1 function reveal concordance of three axes during early determination of left-right asymmetry. *Mech Dev* 125:353–372.
20. Vick P, et al. (2009) Flow on the right side of the gastrocoel roof plate is dispensable for symmetry breakage in the frog Xenopus laevis. *Dev Biol* 331:281–291.
21. Blum M, et al. (2009) Xenopus, an ideal model system to study vertebrate left-right asymmetry. *Dev Dyn* 238:1215–1225.
22. Toyoizumi R, Ogasawara T, Takeuchi S, Mogi K (2005) Xenopus nodal related-1 is indispensable only for left-right axis determination. *Int J Dev Biol* 49:923–938.
23. Sampath K, Cheng AMS, Frisch A, Wright CVE (1997) Functional differences among Xenopus nodal-related genes in left-right axis determination. *Development* 124: 3293–3302.
24. Levin M (2003) Motor protein control of ion flux is an early step in embryonic left-right asymmetry. *Bioessays* 25:1002–1010.
25. Qiu D, et al. (2005) Localization and loss-of-function implicates ciliary proteins in early, cytoplasmic roles in left-right asymmetry. *Dev Dyn* 234:176–189.
26. Adams DS, et al. (2006) Early, H+-V-ATPase-dependent proton flux is necessary for consistent left-right patterning of non-mammalian vertebrates. *Development* 133: 1657–1671.
27. Levin M, Thorlin T, Robinson KR, Nogi T, Mercola M (2002) Asymmetries in H+/K+-ATPase and cell membrane potentials comprise a very early step in left-right patterning. *Cell* 111:77–89.
28. Clark I, Giniger E, Ruohola-Baker H, Jan LY, Jan YN (1994) Transient posterior localization of a kinesin fusion protein reflects anteroposterior polarity of the Drosophila oocyte. *Curr Biol* 4:289–300.
29. Bernstein BW, Bamburg JR (2010) ADF/cofilin: A functional node in cell biology. *Trends Cell Biol* 20:187–195.
30. Gu J, et al. (2010) ADF/cofilin-mediated actin dynamics regulate AMPA receptor trafficking during synaptic plasticity. *Nat Neurosci* 13:1208–1215.
31. Roberts RM, Katayama M, Magnuson SR, Falduto MT, Torres KE (2011) Transcript profiling of individual twin blastomeres derived by splitting two-cell stage murine embryos. *Biol Reprod* 84:487–494.
32. Troemel ER, Sagasti A, Bargmann CI (1999) Lateral signaling mediated by axon contact and calcium entry regulates asymmetric odorant receptor expression in C. elegans. *Cell* 99:387–398.
33. Chang C, Hsieh YW, Lesch BJ, Bargmann CI, Chuang CF (2011) Microtubule-based localization of a synaptic calcium-signaling complex is required for left-right neuronal asymmetry in C. elegans. *Development* 138:3509–3518.
34. Wan LQ, et al. (2011) Micropatterned mammalian cells exhibit phenotype-specific left-right asymmetry. *Proc Natl Acad Sci USA* 108:12295–12300.
35. Xu J, et al. (2007) Polarity reveals intrinsic cell chirality. *Proc Natl Acad Sci USA* 104: 9296–9300.
36. Männer J (2001) Does an equivalent of the "ventral node" exist in chick embryos? A scanning electron microscopic study. *Anat Embryol (Berl)* 203:481–490.
37. Tian T, Zhao L, Zhang M, Zhao X, Meng A (2009) Both foxj1a and foxj1b are implicated in left-right asymmetric development in zebrafish embryos. *Biochem Biophys Res Commun* 380:537–542.
38. Serluca FC, et al. (2009) Mutations in zebrafish leucine-rich repeat-containing six-like affect cilia motility and result in pronephric cysts, but have variable effects on left-right patterning. *Development* 136:1621–1631.
39. Zhao C, Malicki J (2007) Genetic defects of pronephric cilia in zebrafish. *Mech Dev* 124:605–616.
40. Zeng H, Hoover AN, Liu A (2010) PCP effector gene Inturned is an important regulator of cilia formation and embryonic development in mammals. *Dev Biol* 339:418–428.
41. Gardner RL (2010) Normal bias in the direction of fetal rotation depends on blastomere composition during early cleavage in the mouse. *PLoS ONE* 5:e9610.
42. Deinum EE, Tindemans SH, Mulder BM (2011) Taking directions: The role of microtubule-bound nucleation in the self-organization of the plant cortical array. *Phys Biol* 8:056002.
43. Brown NA, Wolpert L (1990) The development of handedness in left/right asymmetry. *Development* 109:1–9.
44. Kuroda R, Endo B, Abe M, Shimizu M (2009) Chiral blastomere arrangement dictates zygotic left-right asymmetry pathway in snails. *Nature* 462:790–794.
45. Carneiro K, et al. (2011) Histone deacetylase activity is necessary for left-right patterning during vertebrate development. *BMC Dev Biol* 11:29.
46. Danilchik MV, Brown EE, Riegert K (2006) Intrinsic chiral properties of the Xenopus egg cortex: an early indicator of left-right asymmetry? *Development* 133:4517–4526.
47. Yost HJ (1991) Development of the left-right axis in amphibians. *Ciba Found Symp* 162:165–176, discussion 176–181.
48. Klar AJ (1994) A model for specification of the left-right axis in vertebrates. *Trends Genet* 10:392–396.
49. Levin M, Nascone N (1997) Two molecular models of initial left-right asymmetry generation. *Med Hypotheses* 49:429–435.
50. Oviedo NJ, Levin M (2007) Gap junctions provide new links in left-right patterning. *Cell* 129:645–647.
51. Mello C, Fire A (1995) DNA transformation. *Methods Cell Biol* 48:451–482.